Universitat Autònoma de Barcelona

MASTER'S THESIS
Modelling for Science and Engineering

THE IMPACT OF URBAN PARKS ON AIR QUALITY

Luis Felipe Diaz Heredia

Supervised by Alba Badia Moragas and Gara Villalba Méndez

Year: 2022-2023
Call: September

Abstract

Improving urban air quality has become one of the main goals of many cities around the world. The addition of new green infrastructure (GI) is seen as one of the most promising strategies in order to improve the air quality, since it may help to decrease the concentration of pollutants in the urban area. In addition, it may help to decrease the temperature and enhance the health and well-being of residents. However, this improvement on the air quality is not guaranteed, the effect is highly context dependent, with models suggesting it may improve air quality in some situations, but be ineffective in others. This project aims to study the impact of urban parks on the air quality over the Metropolitan Area of Barcelona (AMB). The simulations will be performed using the WRF-Chem model. Two model runs (with and without new urban parks) will be compared.

Acknowledgements

This work has been made possible thanks to the support of : Integrated System Analysis of Urban Vegetation and Agriculture (URBAG group), the Barcelona Supercomputing Center (BSC) and the Red Española de Supercomputación (RES), which provided the computer resources at PICASSO. I especially thank Alba Badia Moragas for her continuous support throughout the project from the first steps to the end.

Contents

List of Figures

1 Introduction

The increase of urban areas together with climate change causes serious problems such as an increase in the temperature or a reduction in the air quality in urban areas. These problems may affect both the health and the economy of people living in urban areas. Urban overheating has a great impact on the economy through an increase in the energy demand of buildings. Furthermore, high levels of temperature may increase the mortality [1]. Hence, some researches claim that the health risk is higher in urban areas due to the difference in temperature [2]. In addition, the increase in energy demand causes an increase in harmful pollutants as a side effect of satisfying it. Exposure to these pollutants also has a serious effect on the health of residents of urban areas. Pollutants with the strongest health impact are particulate matter (PM), carbon monoxide (CO), ozone (O_3), nitrogen dioxide (NO_2) and sulphur dioxide ($SO2$). Ambient air pollution urban areas is causing fine particulate matter which result in strokes, heart diseases, lung cancer and chronic respiratory diseases. According to the World Health Organization, outdoor pollution is responsible for about 7 million deaths per year [3]. O_3 is a highly toxic pollutant that strongly affects human health and its concentration increases as a result of intensive urbanization and temperature increase. The NO_2 annual mean limit that the WHO recommends and the legal limit in the UE is 40 μg m^{-3} in the urban air pollution [4]. The origin of these excesses however, lies mostly in emissions from land transport that uses fuels fossils. The highest levels of NO_2 are found in large cities and near major thoroughfares, which is where the most emissions accumulate. The presence of this pollutant is related to the phenomenon of photochemical smog, which consists of episodes of pollution that produce reduced visibility and oxidizing pollutants, thanks to the presence of solar radiation.

Air quality is currently one of the main environmental issues in large cities. Air pollution, mainly caused by NO_2 and fine particles, is now the leading environmental cause of mortality world-wide. High concentrations of pollution may be found in urban areas, due to the high population density and traffic emissions. Urban air quality depends on the characteristics of the atmosphere, such as temperature or chemical processes. Urban air pollution is also influenced by the transport of gaseous and particulate pollutants from surrounding areas.

1.1 Air pollutants and its processes

Air pollution is the contamination of the indoor or outdoor environment by any chemical, physical or biological agent that modifies the natural characteristics of the atmosphere [3]. There are many different types of air pollutants, such as gases, particulates, and biological molecules. Air pollution can cause diseases, allergies, and even death to humans. It may be caused by human activities or natural phenomena.

An air pollutant is a material in the air that can have adverse effects on humans and the ecosystem. The substance may be solid particles, liquid droplets, or gases, and often takes the form of an aerosol. A pollutant can be of natural origin or man-made. Pollutants are classified as primary or secondary. Some pollutants may be both primary and secondary, i.e., they are both emitted directly and formed from other primary pollutants. Primary pollutants are formed and emitted directly from particular sources such as ash from a volcanic eruption or nitrogen oxides from traffic. They include ammonia (NH3), carbon dioxide (CO), Chlorofluorocarbons (CFCs), Nitrogen oxides (NO_x), Volatile organic compounds (VOC), etc.

On the other hand, secondary pollutants are not emitted directly, but they are formed in the lower atmosphere by chemical reactions. High temperatures have also a great effect on urban air quality. Elevated ambient temperatures enhance photochemical reactions with hydrocarbons and generate O_3.

There are two types of pollutant emissions that are released into the atmosphere: biogenic emissions, and fossil emissions (also called anthropogenic emissions) [5]. Both are formed by natural processes, but biogenic emissions contribute to the concentration of air pollutants naturally, whereas fossil fuels need to be burnt. Biogenic sources include emissions from vegetation and soils, but also volcanic emissions, lightning and sea salt. The rise of the temperature may contribute to alter this cycle and thus modify the concentration of these gases in the atmosphere. Most studies focus on surface O_3 [6], [7]. According to these studies, the annual mean concentrations of O_3 have been increasing by on average 0.16 $ppb \cdot year^{-1}$ in cities across the globe over the time period 1995–2014.

O_3 formation is driven by photochemistry reactions between two emitted precursors: NO_x and VOC [8]. It is created when both precursors react in the atmosphere in the presence of sunlight, specifically the UV spectrum. Ambient NO_x and VOC mixing ratios are directly related to the instantaneous rate of production of O_3, and it may be possible to make inferences about the instantaneous production rate of O_3 based on ambient NOx and VOC. Although the O_3 precursors often originate in urban areas, winds may carry O_3 precursors hundreds of kilometres, causing the O_3 formation to occur in less populated regions as well. Its concentration increases as height above sea level increases. Although tropospheric O_3 is less concentrated than stratospheric O_3, it is of concern because of its health effects. Photochemical and chemical reactions involving it fuels many of the chemical activities that occur in the atmosphere during the day and night. It is a pollutant and a component of smog that is produced in large quantities as a result of human activities.

Furthermore, the deposition of a pollutant to a surface involves a permanent loss from the atmosphere, and hence a reduction in its concentration. On the one hand, wet deposition, where atmospheric gases mixed with water in the atmosphere are deposited on all surfaces through precipitation. On the other hand, dry deposition is the free fall to the ground directly from the atmosphere of trace gases and particulate matter. This last one is highly dependent on the characteristics of the surface where it is deposited. The rate of dry deposition may be improved adding GI, reducing the concentration of air pollutants. This rate improvement is determined by the kind of plant species. The surface area of the vegetation and its rate of transpiration may influence on how much the dry deposition rate is improved. This fact makes that the selection of plant species plays an important role determining the pollutant removal achieved thanks to the addition of GI. The rate of dry deposition is proportional to the local concentration of the pollutant[9].

1.2 Green Infrastructure

Green infrastructure (GI) is a term used for a network of green features that are interconnected. They can be defined as a network of natural and semi-natural green spaces such as forests, parks, green roofs and walls that can provide nature-based and cost-effective solutions. Trees contribute to decrease the ambient temperature. They help to cool down the city (maximum reduction seen during night-time) reducing the ambient temperatures in the next day. Therefore, replacing surfaces like asphalt and concrete by vegetation, the stored heat during the day and the emissions during the day and night are seriously reduced. As a result, increasing vegetation fractions may contribute to reduce the ambient temperature.

GI supports human health mainly through urban temperature mitigation and air quality improvements. Several studies aim to evaluate the relationship between health and GI implementation [10], [11], [12]. These articles concluded that there is a significant positive association between health and green spaces around residences. Other articles [12], [13], [14] study the impact of green infrastructure on mortality, morbidity and life expectancy. They find that exists a positive significant correlation between the maximum daily temperature drop (caused by the increase in GI) and the percentage decrease of the heat-related mortality.

Reducing pollutant emissions is the best solution to improve urban air quality. Nevertheless, there are other methods that may contribute to reduce air pollution. One of them is the addition of GI. It relies on the fact that pollutants are absorbed easily by vegetation than other urban surfaces.

Analysis performed in [15] on 55 studies in different cities over the world shows that there is a statistical correlation between the increase in GI and the decrease in peak ambient temperatures. In particular, when the GI fraction reaches its maximum, it shows that the average peak temperatures can be reduced by a maximum of 1.8ºC during the day and 2.3ºC at night. The increase of the GI is limited due to the little space available that may be in a city. However, an increase of the 20 % in the GI may decrease the peak temperature in 0.3ºC during the day and 0.5ºC during the night.

However, the effectiveness evidence of the use of GI to improve air quality is weak. In addition, depending on thermal conditions, vegetation causes an indirect increase of O_3 concentration via the emission of biogenic VOC (BVOC). The impact of GI on air quality may oscillate a lot in different situations. Sometimes, models suggest that GI may improve urban air quality in some situations, but be ineffective or even detrimental in others. This last situation may be due to the concept of 'urban canopy'. It refers to the influence of the volume-filling effects of buildings and trees in the air transport resulting on the dispersion of air pollutants. GI are semi-permeable obstacles to the air flow that may introduce a perturbation on its direction and turbulence. Depending on the tree morphology, these effects may vary a lot.

Increase of GI is associated with multiple dynamic and chemical changes in the lower atmosphere. Vegetation accumulates particulate matter by sedimentation, while it also absorbs gaseous pollutants such as NO_x and O_3. As said before, increase of GI results in lower ambient and surface temperatures, which may have either a positive or negative impact on pollutant concentration. Besides temperature reduction, trees may decrease wind speed in the built environment, increasing the concentration of pollutants in the urban canyons and canopies, while it may affect the transport of pollutants in the city.

1.3 Urban heat island

"Urban heat islands" are urban areas that are significantly warmer than their surrounding rural areas due to human activities. They occur when cities replace natural land cover with dense concentrations of pavement, buildings, and other surfaces that absorb and retain heat. The temperature difference is usually larger at night than during the day, and is most apparent when winds are weak. This effect has an impact on energy costs, air quality, and heat-related illness and mortality. It is most noticeable during the summer and winter. A study has shown that heat islands can be affected by proximity to different types of land cover, so that proximity to barren land causes urban land to become hotter and proximity to vegetation makes it cooler [16].

Not all cities have a distinct urban heat island, and the heat island characteristics depend strongly on the background climate of the area. To reduce the urban heat island effect, the main strategies are planting trees in cities, white roofs and light-coloured concrete, green infrastructure and passive daytime radiative cooling. Climate change is not the cause of urban heat islands, but it is causing more frequent and more intense heat waves which in turn amplify the urban heat island effect in cities.

2 WRF-Chem Model

2.1 Numerical weather forecasting models

Numerical weather forecasting models are the fundamental tool of any weather forecast. Specifically, numerical weather prediction consists of simulating the future evolution of meteorological variables that determine the state of the atmosphere by using mathematical models. These models are formulated from the physical laws that explains the behaviour of the atmosphere and constitute a system of equations that, given their complexity, can only be solved approximately by using computers.

Although the atmosphere is a continuous medium, these equations can only be solved at discrete points in order for the calculation to be feasible. All these points together form a three-dimensional mesh. Thus, as the distance between these points (mesh step) decreases, the model is able to explicitly simulate smaller scale weather phenomena and thus has higher resolution. In return, this involves increasing the simulation's calculation time.

On the other hand, the effects of the physical processes that numerical models are not able to solve are estimated by parameterizations; that is, a set of mathematical formulae that attempt to roughly represent smaller scale phenomena. Although all weather models are based on the same physical laws, there are differences in both their mathematical formulation and the numerical techniques used to solve the system of equations. In addition, they are also distinguished depending on the geographic area (or domain) they encompass: in global models, the three-dimensional mesh covers the entire planet while limited area models comprise only one particular area.

2.2 Air Quality Models

Air quality modelling (AQM) uses mathematical and numerical techniques to simulate the physical and chemical processes that affect air pollutants as they disperse and react in the atmosphere. AQMs use inputs emissions and meteorological data from nearby weather stations such as wind speed and direction to obtain air quality data. They are designed to characterize primary pollutants emitted directly into the atmosphere and, in some cases, secondary pollutants that are formed as a result of complex chemical reactions within the atmosphere. AQM is a common and reliable data source to estimate air quality impacts from emission sources. AQM is also used to predict future impacts from proposed emission sources as well as anticipated growth in urban areas. Air monitoring refers to measuring pollutants in the air we breathe, and it is a widely used method of obtaining quality assured air quality data.

AQM may be preferred over air monitoring for several reasons. For instance, air monitoring is more expensive to install and maintain samplers and instruments. In addition, collecting monitoring data for an analysis takes time, from months to years, and results are limited to some specific location. They are widely used by agencies in order to control air pollution. Their main uses are to identify source contributions to air quality problems and assist in the design of effective strategies to reduce harmful air pollutants. AQMs may be used to predict future air pollutant concentrations from multiple sources after the implementation of a new project that modifies the area where the study is performed, in order to estimate the effectiveness of the program in reducing harmful exposures to humans and the environment.

2.3 WRF-Chem Model

The Weather Research and Forecasting (WRF) Model is an atmospheric modelling system designed for both research and numerical weather prediction. It is an open-source community model. WRF development began in the latter half of the 1990's. It was developed through a partnership of the National Center for Atmospheric Research (NCAR), the National Oceanic and Atmospheric Administration (NOAA), the United States Air Force, the Naval Research Laboratory, the University of Oklahoma, and the Federal Aviation Administration. In addition, for prediction needs beyond basic weather forecasting, WRF supports a number of tailored capabilities, including WRF-Chem (atmospheric chemistry), WRF-Hydro (hydrological modelling), and WRF-Fire (wildland fire modelling).

WRF-Chem is the Weather Research and Forecasting (WRF) model coupled with Chemistry. The model simulates the emission, transport, mixing, and chemical transformation of trace gases and aerosols simultaneously with the meteorology. It has as inputs meteorology and chemistry data (usually from another simulation) as well as emissions and geography data. The model simulates the physical process together wit chemical mechanisms. Typically, it requires emission source maps as additional inputs.

The boundary conditions are provided by another simulation of a larger scale domain. A nest is a finer-resolution model run. It may be embedded simultaneously within a parent model run, or run independently as another model forecast. The nest covers a portion of the parent domain, and is driven along its lateral boundaries by the parent domain. This procedure is needed in order to achieve higher resolutions in the inner domain, which is the one we are interested in. Higher resolution domains require more computational, as a shorter time step is used.

Initial conditions for real-data cases are pre-processed through a separate package called the WRF Preprocessing System (WPS). The WPS is a set of programs that take terrestrial and meteorological data (typically in GRIB format) and transforms them for input to the WRF pre-processor program for real-data cases. These programs are:

- `geogrid`: interpolates static geographical data to the WRF grids.
- `ungrib`: extracts meteorological fields from GRIB-formatted files

- `metgrid`: interpolates the meteorological data horizontally onto your model domain. Output from metgrid.exe is used as input to WRF (through the real.exe program).

The files prepared by this set of programs will be used to generate the input data of the model.

WRF provides the capability to focus the area of a simulation via nesting options. It allows a resolution to be enhanced over a region of interest by introducing an additional grid (or grids) into the simulation. This subdomain with increased horizontal resolution is completely contained within the parent domain. The subdomain is commonly referred to as the child domain.

3 Study Case

This project aims to study the impact of urban parks on the air quality over the Metropolitan Area of Barcelona (AMB). The simulations are performed for the period July 01, to July 26, 2015. The reference scenario is a simulation using the WRF-Chem model in the AMB with the current GI data as input. This may be used to compare with the experimental data measured of the air quality in the AMB during the selected period. Then, the second simulation adds some possible future urban parks that may be developed in the AMB. The goal is to compare the impact in the air quality after adding some urban parks. The urban parks of both scenarios can be seen in the Figure 1.

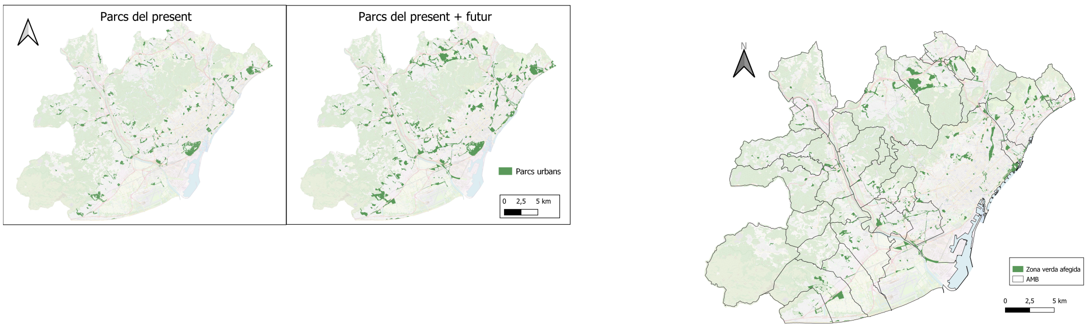

(a) (b)

Figure 1: Urban Parks in the AMB of both simulations, (a) Comparison of before and after adding urban parks and (b) Future added urban parks (source URBAG group, `https://urbag.eu/`)

The AMB is the second most populated urban area in Spain. It is located in Catalonia in the northeastern region of Spain. The Mediterranean climate prevails in the region, with dry and hot summers and clear skies. The most problematic pollutants in the city are O_3, PM_{10}, and NO_2, thus Barcelona annually reports one of the highest air pollution levels in Europe. In particular, in 2015, there was a general increase of 11 % in the annual mean levels of NO_2 compared to the previous year. These levels exceeded the WHO guideline (40 $\mu g\, m^{-3}$) in the urban air pollution ground monitoring stations of Eixample, Gràcia-Sant Gervasi, Poblenou and Ciutadella [17]. Regarding PM_{10}, there has been a general increase of 13 % in the mean average levels of PM10 compared to the previous year. These levels exceeded the WHO guideline (20 $\mu g\, m^{-3}$) in all stations. Finally, O_3 levels meet the target value established by the EU (180 $\mu g\, m^{-3}$). Since 2003, maximum hourly ozone levels have not exceeded the threshold. However, in 2015 there was an exceed at the urban station of Ciutadella.

As we can see in the Figure 2, Barcelona, facing the Mediterranean to the southeast, is located on a plain generally confined by the Besós River (north), the Llobregat River (south), the rocky outcrop of Montjuich , and the semicircle of mountains of which Tibidabo is the highest point. Although Barcelona is sometimes windy, its protective semicircle of mountains shields it from the harsh, cold winds that blow out of the north and west. The two main rivers in the area flow perpendicular to the sea and play an important role in the creation of air-flow patterns [18].

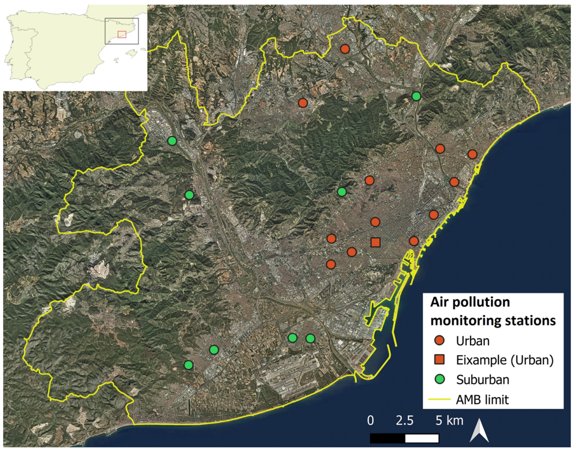

Figure 2: Topographic area of Barcelona [19]

The Figure 3 shows the difference between the vegetation fraction in both scenarios. As we can see, there is a relevant increase in the east area of the AMB. There is a maximum increase of 16.2 % in the urban vegetation fraction. The new vegetation is mainly concentrated around the Besos and Llobregat rivers.

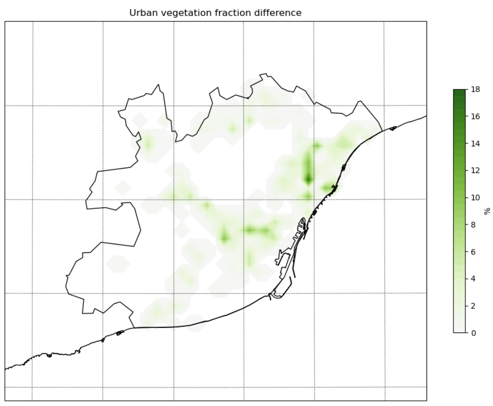

Figure 3: Urban Vegetation fraction difference between both scenarios (difference between the simulation with new parks and the reference scenario).

4 Model Setup

The model setup was designed by the URBAG group (https://urbag.eu/) and a similar configuration has been used in previous studies [19] [20]. One month simulation covering the Iberian Peninsula with a 9km x 9km (domain 1, D1) resolution was run to provide the initial and boundary conditions (ICs/BCs) for the other domains (D2 and D3, 3km and 1km resolution, respectively) for the two runs. The meteorological and chemical IC/BCs were determined using the ERA5 global model data [21] and WACCM [22], respectively. The HERMESv3 preprocessor tool [23] was used to create the anthropogenic emissions files from the CAMS-REG-APv3.1 database [24] for the D1 domain. This emission inventory is based on data from 2016. Anthropogenic emissions files for D2 and D3 were provided by the Barcelona Supercomputing Center using the HERMES bottom–up module emissions model [25]. Biogenic emissions are computed online from the Model of Emissions of Gases and Aerosols from Nature v2 (MEGAN [26]). All model input data to run the model were prepared by the URBAG group.

The simulation of the reference scenario has been validated by the URBAG group with several air quality observations from the Xarxa de Vigilància i Previsió de la Contaminació Atmosfèrica (XVPCA) over the AMB for NO_2 and O_3. The model shows a good agreement with the observations during the period of July 2015 (correlation between 0.1-0.57 and 0.55-0.63, for NO_2 and O_3, respectively) although there are specific biases over the urban stations representing high traffic. However, the model exhibits low biases at stations located in a low traffic area. Surface NO_2 and O_3 concentrations are very sensitive to the emissions, therefore, these model biases are mostly due to the our emission inventory and the resolution of our model (1km) that is not able to capture traffic hotspots.

5 Results and Discussion

5.1 Physical Variables

In this section, we will discuss the impact of the GI increase in some physical variables such as the Temperature at 2m and the wind speed.

5.1.1 Temperature at 2m (T2)

In the Figure 4, it is shown the difference between both simulations (difference between the simulation with new parks and the reference scenario) of the Temperature at 2m. Red colors represent an increase in the simulation values with new parks added compared to the other, while blue colors represent a decrease. The comparison between the two simulations shows that the impact of adding more urban parks to the AMB implies, on average, a maximum temperature reduction of 0.39 ºC in the period from 00:00 to 06:00 and of 0.35 ºC the rest of the day. As we can see, most of the reductions are located nearby the regions where the urban vegetation fraction increased (see in Figure 3). The increases in the temperature are located in the north-west area of the AMB.

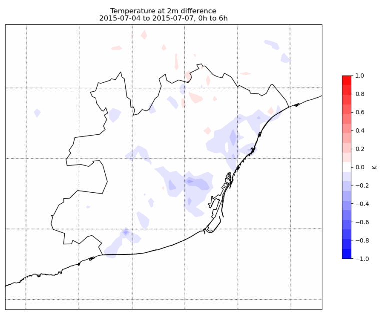

(a) 0h to 6h

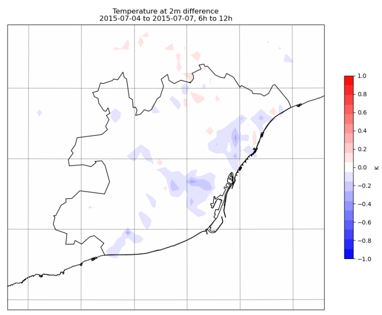

(b) 6h to 12h

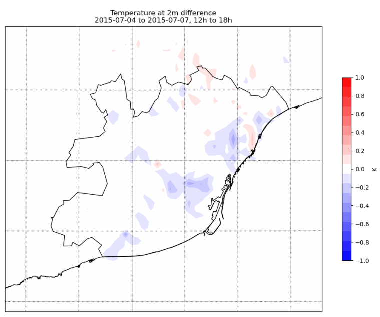

(c) 12h to 18h

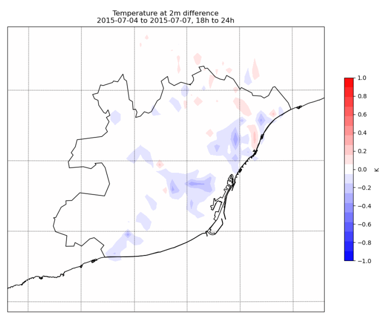

(d) 18 h to 00h

Figure 4: Mean temperature at 2m differences in 4 periods of 6 hours over 4 days

The greatest drop in temperature at 2m is detected on 2015-07-04, from 12h to 18h and corresponds to -0.716 ºC. On the other hand, the largest increase is detected on 2015-07-07 from 18h to 24h and corresponds to 0.975 ºC. The plots corresponding to these periods can be seen in the Figure 5. The increase/decrease in the temper-

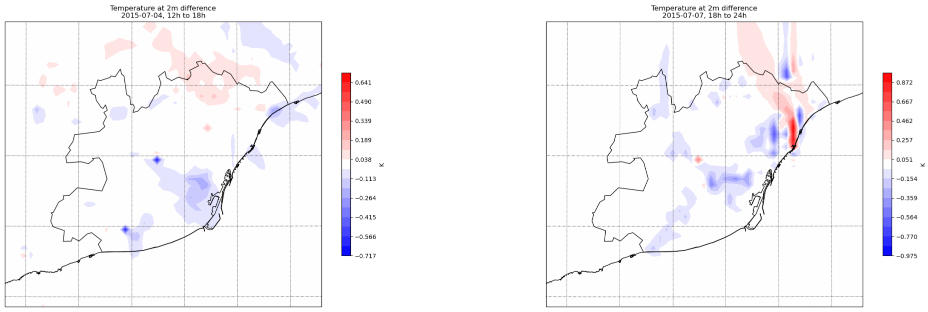

(a) 2015-07-04, from 12h to 18h (b) 2015-07-07 from 18h to 24h

Figure 5: Temperature at 2m differences in the periods of the largest increase and decrease

ature may be also influenced by the change in the land use category between both scenarios. For instance, if we changed from forest to urban park then we may see an increase in temperature. On the other hand, if we changed from urban areas to urban park then we may see a reduction. However, the influence of the land use category should be studied in more detail in the future, since its effect could be more complex.

5.1.2 Wind Speed

In the Figure 6, it is shown the difference between both simulations (difference between the simulation with new parks and the reference scenario) of the wind speed. Red colors represent an increase in the simulation values with new parks added compared to the other, while blue colors represent a decrease. As we can see, wind speed mostly increases. The comparison between the two simulations shows that the impact of adding more urban parks to the AMB implies, on average, a maximum wind speed increase of 0.5 m/s to 0.6 m/s for the whole day. As we can see, these increases are located nearby the regions where the urban vegetation fraction increased (see in Figure 3).

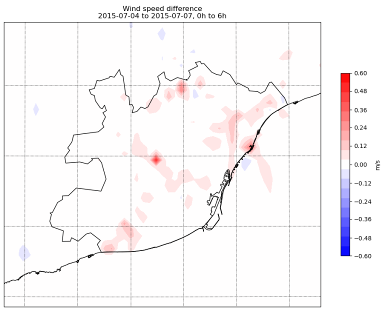

(a) 0h to 6h

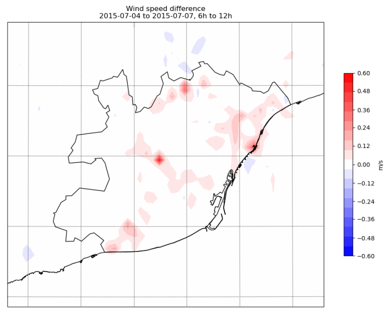

(b) 6h to 12h

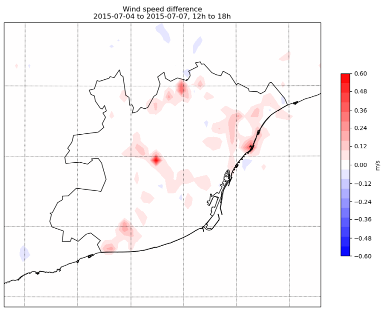

(c) 12h to 18h

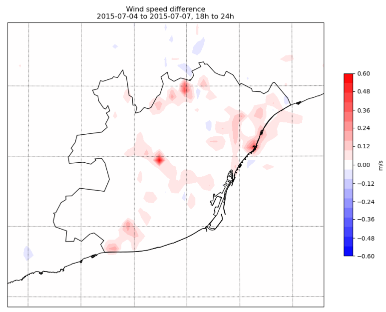

(d) 18h to 00h

Figure 6: Mean wind speed differences in 4 periods of 6 hours over 4 days

The greatest increase in the wind speed is predicted on 2015-07-07, from 6h to 12h and corresponds to 0.95 m/s. On the other hand, the largest reduction is during the same period and corresponds to -0.54 m/s. The plots corresponding to these periods can be seen in the Figure 7.

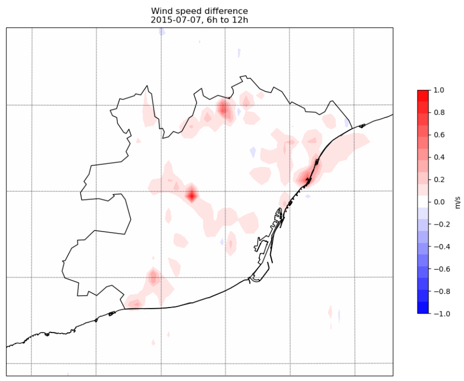

Figure 7: Wind speed difference in the period of the largest increase and decrease, 2015-07-07, from 6h to 12h

Again, the land uses may have an influence on the wind speed. When we remove urban areas to make parks, the sea breeze increases. This may be due to the temperature difference between sea and land, increasing the pressure difference between land and sea, enhancing the development of the sea breezes [27].

5.2 Chemical variables

In this section, we will discuss the impact of the GI increase in some chemical variables, the concentration of some pollutants such as NO_2 and 0_3. Air quality depends not only on the emission of pollutants from different sources, but also on the meteorological conditions. The concentrations of pollutants are affected by changes in the physical parameters (wind speed and temperature) and changes in the chemical processes such as the deposition and biogenic emissions from the urban parks.

Wind is responsible for the dispersion of pollutants, depending on its direction and intensity, can disperse the pollutants or concentrate them on a reduced geographical area. Temperature affects the chemistry of pollutants as well as their emissions. Cold temperatures reduce the volatility of certain gases but increase automobile emissions due to less efficient combustion. On the other hand, hot temperatures enhance the photochemical reactions.

In atmospheric chemistry, the concentrations of NO, NO_2 and O_3 are related. The conversion of NO to NO_2 mainly occurs through oxidation by O_3.The conversion happens quickly, so it can be assumed as instantaneous, although the reaction rate can be from tens of seconds to a few minutes, depending on availability of reactants such as O_3 and volatile organic compounds (VOCs), solar energy, and ambient meteorological conditions.

5.2.1 Nitrogen dioxide (NO_2)

In the Figure 8, we can see that NO_2 levels mainly decreased. Again, most of the reductions are located in the regions where the urban vegetation fraction increases and their surroundings. Both the greatest increase and the greatest decrease in the mean concentration difference are detected in the first time slot and corresponds to -1.674 ppb and 0.994 ppb respectively.

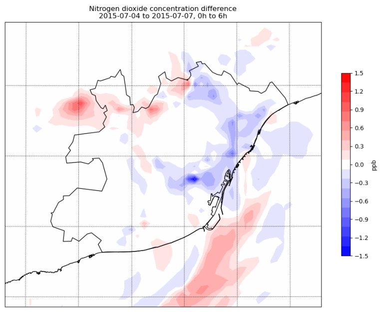

(a) 0h to 6h

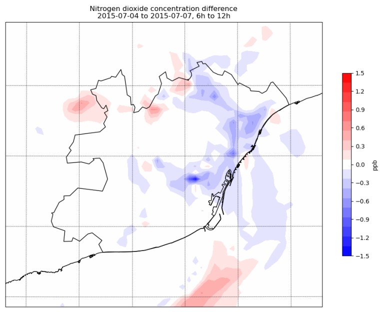

(b) 6h to 12h

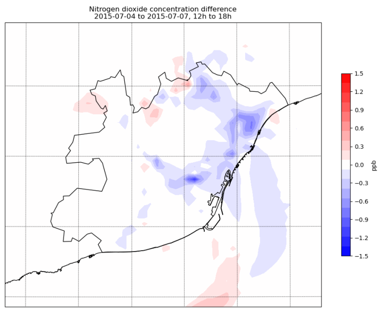

(c) 12h to 18h

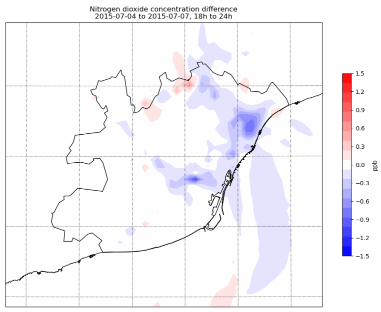

(d) 18h to 00h

Figure 8: Mean NO_2 concentration differences in 4 periods of 6 hours over 4 days expressed in parts by billion (ppb)

The greatest increase in the NO_2 concentration is predicted on 2015-07-04, from 0h to 6h and corresponds to 3.975 ppb. On the other hand, the largest reduction is detected on 2015-07-04 from 18h to 24h and corresponds to -3.978 ppb. The plots corresponding to these periods can be seen in the Figure 9.

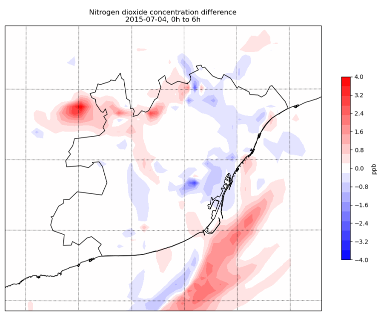

(a) 2015-07-04, from 0h to 6h

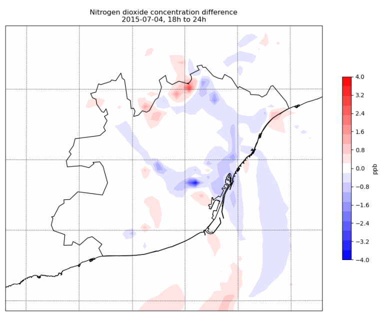

(b) 2015-07-04 from 18h to 24h

Figure 9: NO_2 concentration differences in the periods of the largest increase and decrease

5.2.2 Nitrogen oxide (NO)

In the Figure 10, we can see that NO levels mainly decreased. Again, most of the reductions are located in the regions where the urban vegetation fraction increases and their surroundings. Both the greatest increase and the greatest decrease in the mean concentration difference are detected in the first time slot and corresponds to -1.383 ppb and 1.332 ppb respectively.

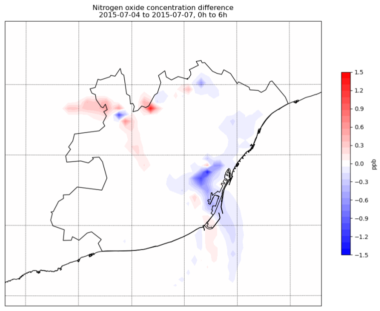

(a) 0h to 6h

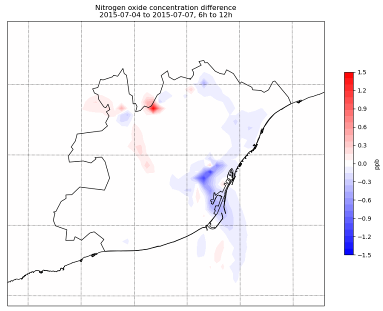

(b) 6h to 12h

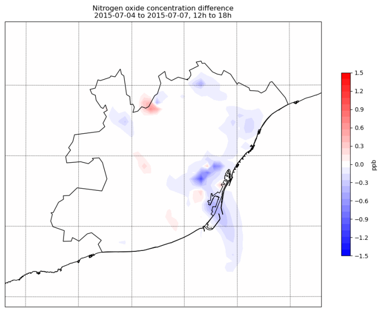

(c) 12h to 18h

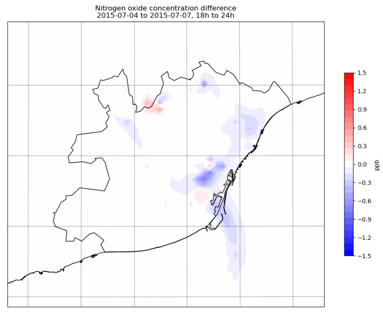

(d) 18h to 00h

Figure 10: Mean NO concentration differences in 4 periods of 6 hours over 4 days expressed in parts by billion (ppb)

The greatest increase in the NO concentration is predicted on 2015-07-04, from 06h to 12h and corresponds to 5.755 ppb. On the other hand, the largest reduction is detected on 2015-07-04 from 00h to 06h and corresponds to -4.684 ppb. The plots corresponding to these periods can be seen in the Figure 11.

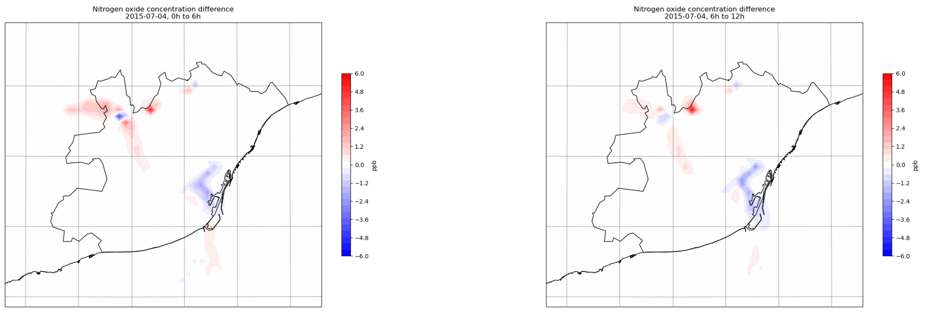

(a) 2015-07-04, from 0h to 6h

(b) 2015-07-04 from 06h to 12h

Figure 11: NO concentration differences in the periods of the largest increase and decrease

5.2.3 Ozone (O_3)

In the Figure 12, we can see the difference between both scenarios (difference between the simulation with new parks and the reference scenario) of the O_3 concentration. Again, most of the reductions are located in the regions where the urban vegetation fraction increases and their surroundings. Both the greatest increase and the greatest decrease in the mean concentration difference are detected in the first time slot and corresponds to -0.783 ppb and 1.265 ppb respectively.

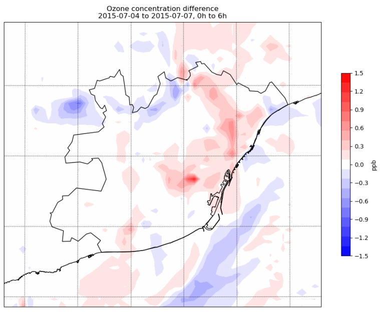

(a) 0h to 6h

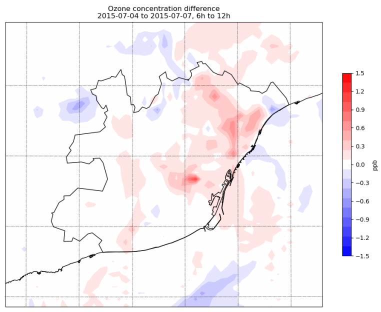

(b) 6h to 12h

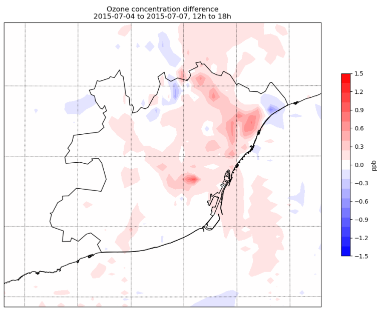

(c) 12h to 18h

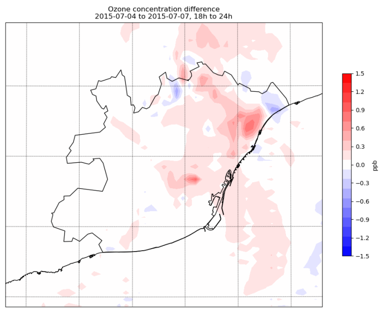

(d) 18h to 00h

Figure 12: Mean O_3 concentration differences in 4 periods of 6 hours over 4 days expressed in parts by billion (ppb)

The greatest increase in the O_3 concentration is predicted on 2015-07-06, from 0h to 6h and corresponds to 3.221 ppb. On the other hand, the largest reduction is detected on 2015-07-04 from 0h to 6h and corresponds to -3.064 ppb. The plots corresponding to these periods can be seen in the Figure 13.

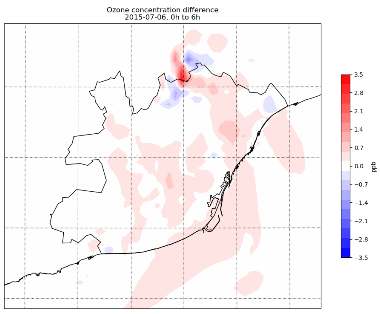

(a) 2015-07-06, from 0h to 6h

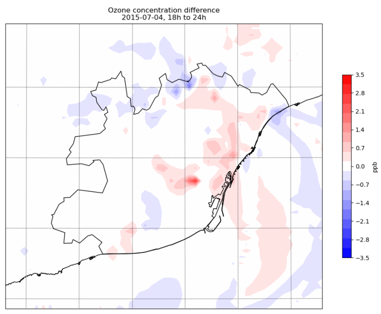

(b) 2015-07-04 from 0h to 6h

Figure 13: O_3 concentration differences in the periods of the largest increase and decrease

Since NO_x species are O_3 precursors, we would expect a positive relation between NO_x and O_3 concentrations, i.e., if one decreases the other should too. However, NO is an important depressor of O_3 during the night through the process of NO_x titration. This consists of the removal of O_3 through reaction with NO ($NO + O_3 \rightarrow NO_2 + O_2$). On the one hand, decreasing NO reduces the amount of O_3 reduced through NO_x titration, leading to an increase in O_3 concentrations. On the other hand, decreasing NO_2 reduces the amount of O_3 formed by chemical reactions between NO_2 and VOCs. The results suggest that the two mechanisms combined have led the system to an increase of O_3 concentrations. However, to fully understand why O_3 has increased we also need to look at what has happened to VOCs, because if the concentration of VOCs increases the formation of O_3 will also increase.

6 Conclusion

In this project, we used the WRF-Chem model to analyse the air quality impact over the AMB due to the addition of new GI in the area. The results show a global reduction in the temperature in the AMB, especially in those regions where the urban vegetation fraction was increased. However, there is a general increase in the temperature for the northeast part of the AMB. This may be due to the change in the land uses, if we change from forest to urban park then we may see an increase in temperature. Regarding the wind speed, we saw a general increase probably due to the change in the land uses. The exchange of urban areas for parks causes an increase in sea breezes, i.e., the wind speed increases in those regions. However, the land uses that produce this change and its impact could be further developed in a future study.

We also saw a general reduction in the concentrations of NO and NO_2. Therefore, we would expect a reduction in the O_3 concentration, since they are O_3 precursors. However, we found a general increase in the O_3 concentration. This result may be explained from the NO_x titration, which is a process that consists in the removal of O_3 through reaction with NO. Therefore, we may conclude that the reduced O_3 production is overwhelmed by the reduction on NO_x titration, resulting in a net increase in the O_3 concentration. However, to fully understand why O_3 has increased we also need to look at what has happened to VOCs, as if the concentration of VOCs increases the formation of O3 will also increase.

As a result, the impact of the new GI added to the AMB could help to slightly reduce the maximum temperature in the areas close to these new parks. At the same time, it increases the wind speed and it also helps to reduce the NO_x concentrations. However, more effective O_3 mitigation strategies are needed.

Future studies may focus on studying the impact of the different land uses on the different physical and chemical variables. In addition, another possible line of study could be how chemical processes such as dry deposition and biogenic emissions change, together with their effect on air quality in these scenarios with the new GI added.

References

[1] Helen Johnson et al. “The impact of the 2003 heat wave on mortality and hospital admissions in England”. In: *Health statistics quarterly / Office for National Statistics* 25 (Feb. 2005), pp. 6–11.

[2] Leah Schinasi, Tarik Benmarhnia, and Anneclaire De Roos. “Modification of the association between high ambient temperature and health by urban microclimate indicators: A systematic review and meta-analysis”. In: *Environmental research* 161 (Nov. 2017), pp. 168–180. DOI: 10.1016/j.envres.2017.11.004.

[3] World Health Organization. *Air pollution.* URL: https://www.who.int/health-topics/air-pollution#tab=tab_1.

[4] World Health Organization. *Air quality guidelines: global update 2005: particulate matter, ozone, nitrogen dioxide and sulfur dioxide.* URL: https://apps.who.int/iris/handle/10665/107823.

[5] Toitū Envirocare. *Explainer Series — Why Biogenic emissions matter.* URL: https://www.toitu.co.nz/news-and-events/news/ems/explainer-series-why-biogenic-emissions-matter.

[6] Joakim Langner, Robert Bergström, and Valentin Foltescu. “Impact of climate change on surface ozone and deposition of sulphur and nitrogen in Europe”. In: *Atmospheric Environment* 39 (Feb. 2005), pp. 1129–1141. DOI: 10.1016/j.atmosenv.2004.09.082.

[7] Pierre Sicard et al. “Should we see urban trees as effective solutions to reduce increasing ozone levels in cities?” In: *Environmental Pollution* 243 (Dec. 2018), pp. 163–176. DOI: 10.1016/j.envpol.2018.08.049.

[8] University of Michigan Dr. Sanford Sillman. *Overview: Tropospheric ozone, smog and ozone-NOx-VOC sensitivity.* URL: http://www-personal.umich.edu/~sillman/ozone.htm#OZ01.2.

[9] Arvind Tiwari et al. “Considerations for evaluating green infrastructure impacts in microscale and macroscale air pollution dispersion models”. In: *Science of The Total Environment* 672 (Mar. 2019), pp. 410–426. DOI: 10.1016/j.scitotenv.2019.03.350.

[10] Francesco Nardo, Rosella Saulle, and Giuseppe La Torre. “Green areas and health outcomes: A systematic review of the scientific literature”. In: *Italian Journal of Public Health* 7 (Dec. 2010), pp. 402–413. DOI: 10.2427/5699.

[11] Rod Simpson et al. “The short-term effects of air pollution on daily mortality in four Australian cities”. In: *Australian and New Zealand journal of public health* 29 (July 2005), pp. 205–12. DOI: 10.1111/j.1467-842X.2005.tb00758.x.

[12] Magdalena Berg, Wanda Wendel-Vos, Mireille van Poppel, Willem Mechelen, and Jolanda Maas. “Health Benefits of Green Spaces in the Living Environment: A Systematic Review of Epidemiological Studies”. In: *Urban Forestry Urban Greening* 14 (Aug. 2015). DOI: 10.1016/j.ufug.2015.07.008.

[13] Sharon Harlan, Juan Declet-Barreto, William Stefanov, and Diana Petitti. "Neighborhood Effects on Heat Deaths: Social and Environmental Predictors of Vulnerability in Maricopa County, Arizona". In: *Environmental health perspectives* 121 (Nov. 2012). DOI: 10.1289/ehp.1104625.

[14] Elissa Wilker et al. "Green Space and Mortality Following Ischemic Stroke". In: *Environmental research* 133C (June 2014), pp. 42–48. DOI: 10.1016/j.envres.2014.05.005.

[15] Mat Santamouris and Paul Osmond. "Increasing Green Infrastructure in Cities: Impact on Ambient Temperature, Air Quality and Heat-Related Mortality and Morbidity". In: *Buildings* 10 (Dec. 2020), p. 233. DOI: 10.3390/buildings10120233.

[16] Mohammad Mansourmoghaddam et al. "Study and prediction of land surface temperature changes of Yazd city: Assessing the proximity and changes of land cover". In: 12 (May 2021), pp. 1–27.

[17] Agència de Salut Pública de Barcelona. "Avaluació de la qualitat de l'aire a la ciutat de Barcelona". In: (2015). URL: https://www.aspb.cat/wp-content/uploads/2016/10/Informe_Qualitat_Aire_2015.pdf.

[18] Jordi Massagué et al. "2005–2017 ozone trends and potential benefits of local measures as deduced from air quality measurements in the north of the Barcelona Metropolitan Area". In: *Atmospheric Chemistry and Physics* 19 (Feb. 2019), pp. 7445–7465. DOI: 10.5194/acp-19-7445-2019.

[19] Alba Badia et al. "A take-home message from COVID-19 on urban air pollution reduction through mobility limitations and teleworking". In: 1 (Aug. 2021), p. 10. DOI: 10.1038/s42949-021-00037-7.

[20] A. Badia et al. "Modelling the impacts of emission changes on O_3 sensitivity, atmospheric oxidation capacity and pollution transport over the Catalonia region". In: *EGUsphere* 2023 (2023), pp. 1–38. DOI: 10.5194/egusphere-2023-160. URL: https://egusphere.copernicus.org/preprints/2023/egusphere-2023-160/.

[21] Hans Hersbach et al. "The ERA5 global reanalysis". In: *Quarterly Journal of the Royal Meteorological Society* 146.730 (2020), pp. 1999–2049. DOI: https://doi.org/10.1002/qj.3803. eprint: https://rmets.onlinelibrary.wiley.com/doi/pdf/10.1002/qj.3803. URL: https://rmets.onlinelibrary.wiley.com/doi/abs/10.1002/qj.3803.

[22] A. Gettelman et al. "The Whole Atmosphere Community Climate Model Version 6 (WACCM6)". In: *Journal of Geophysical Research: Atmospheres* 124.23 (2019), pp. 12380–12403. DOI: https://doi.org/10.1029/2019JD030943. eprint: https://agupubs.onlinelibrary.wiley.com/doi/pdf/10.1029/2019JD030943. URL: https://agupubs.onlinelibrary.wiley.com/doi/abs/10.1029/2019JD030943.

[23] M. Guevara, C. Tena, M. Porquet, O. Jorba, and C. Pérez Garcıa-Pando. "HERMESv3, a stand-alone multi-scale atmospheric emission modelling framework – Part 1: global and regional module". In: *Geoscientific Model Development* 12.5 (2019), pp. 1885–1907. DOI: 10.5194/gmd-12-1885-2019. URL: https://gmd.copernicus.org/articles/12/1885/2019/.

[24] C. Granier et al. "The Copernicus Atmosphere Monitoring Service global and regional emissions (April 2019 version)". In: (2019). DOI: https://doi.org/10.24380/D0BN-KX16.

[25] M. Guevara, C. Tena, M. Porquet, O. Jorba, and C. Pérez Garcıa-Pando. "HERMESv3, a stand-alone multi-scale atmospheric emission modelling framework – Part 2: The bottom–up module". In: *Geoscientific Model Development* 13.3 (2020), pp. 873–903. DOI: 10.5194/gmd-13-873-2020. URL: https://gmd.copernicus.org/articles/13/873/2020/.

[26] A. B. Guenther et al. "The Model of Emissions of Gases and Aerosols from Nature version 2.1 (MEGAN2.1): an extended and updated framework for modeling biogenic emissions". In: *Geoscientific Model Development* 5.6 (2012), pp. 1471–1492. DOI: 10.5194/gmd-5-1471-2012. URL: https://gmd.copernicus.org/articles/5/1471/2012/.

[27] Ricard Segura et al. "Sensitivity study of PBL schemes and soil initialization using the WRF-BEP-BEM model over a Mediterranean coastal city". In: *Urban Climate* 39 (Sept. 2021), p. 100982. DOI: 10.1016/j.uclim.2021.100982.